NANOFIBRILLATED CELLULOSE AEROGEL FROM KHAT (*CATHA EDULIS*) WASTE: FABRICATION AND CHARACTERIZATIONS

JEMAL DILEBO, TESFAYE GABRIEL and KEBEDE WONDU

Department of Pharmaceutics and Social Pharmacy, School of Pharmacy, College of Health Sciences, Addis Ababa University, Addis Ababa, Ethiopia
✉ *Corresponding author: J. Dilebo, jemal.dilebo@aau.edu.et*

Received March 7, 2023

Cellulose fiber was extracted from khat waste (KW) using the chlorine free method and an aerogel was prepared by freeze drying of nanofibrillated cellulose of KW. The aerogel was loaded with a model drug, diclofenac sodium. The drug loaded aerogel (LA), drug unloaded aerogel (ULA), as-extracted cellulose (Cel) and KW were characterized using different instrumental techniques. Nanofibrillation of the cellulose fiber for 4 h gave 83.06% nanofiber. ULA had lower crystallinity index, as compared to Cel (53.89% *vs* 65.22%), but had higher thermal stability than LA and Cel. The drug loading capacity of the aerogel was 11.7 mg of pure drug per 100 mg of the nanofiber. The *in vitro* drug release from LA was less than one-third of the loaded drug (*i.e.*, 31.4%) within 6 h. The findings highlight that nanofibrillated cellulose aerogel can be prepared from KW and may have potential applications in areas such as drug delivery.

Keywords: nanofibrillated cellulose, cellulose, aerogel, khat waste

INTRODUCTION

Aerogels are materials made by substituting the liquid solvent in a gel by air without significantly changing the network structure or the volume of the gel body.[1] Aerogels have unique characteristics, such as low density, high specific surface area, and high porosity.[2] Aerogels can be synthesized from inorganic materials (*e.g.*, SiO_2, TiO_2, SnO_2, V_2O_5, and Al_2O_3), synthetic polymers (*i.e.*, resorcinol–formaldehyde, polyvinylchloride, polypropylene, and polyimide), biopolymers (alginate, proteins, chitosan, and hemicellulose), and carbon (*i.e.*, carbon, carbon nanotubes, and graphene).[3,4]

Aerogels have been investigated for potential applications in thermal insulation, acoustic insulation, batteries, storage of rocket fuels, confining radioactive wastes, gas filters, dielectric materials, cosmic dust collection, waste water treatment, nuclear waste storage, catalysis, and biomedical products.[5]

Cellulose based aerogels can be fabricated from regenerated cellulose, cellulose derivatives and natural celluloses (nanocellulose and bacterial cellulose). Cellulose aerogels have comparable density, porosity, and specific surface area to silica aerogels and synthetic polymer aerogels, but cellulose aerogels have superior compressive strength and biodegradability.[3]

Fabrication of aerogels from abundant and renewable resources, such as Khat waste cellulose, is important to reduce the reliance on non-renewable resources such as silica, alumina and carbon precursors. Khat (*Catha edulis*) waste is produced after taking the shoots of Khat during chewing for recreational purpose by millions in Ethiopia. The waste is mainly composed of twigs. This waste is becoming an environmental burden in urban places in Ethiopia. In the present study, an aerogel was fabricated from nanofibrillated khat cellulose by freeze drying. The aerogel was characterized and used as a drug carrier system for diclofenac sodium; the release of the loaded drug was also evaluated.

EXPERIMENTAL

Materials

Fresh khat waste (KW) was collected from khat shops in Addis Ababa, Ethiopia, and washed with tap water, ground with a cutter machine and dried in open air. Glacial acetic acid (Riedel-de Haën), formic acid 98% (Central Drug House Ltd., New Delhi, India), sulfuric acid 97% (BDH, England), hydrogen peroxide 50% (Awash Melkassa, Ethiopia), sodium hydroxide

99.8% (Ranchem Industry), diclofenac sodium (Healthcare Limited PLC, India), were used as received.

Methods

Cellulose extraction

Cellulose fiber was extracted from KW according to the method of Gabriel *et al*.,[6] with slight modification. Initial pretreatment of KW was made with a mixture of 40% formic acid and 40% acetic acid (7:3 ratio) on a hot plate at 90 °C for 1.5 h. Then followed a treatment with a mixture of 40% formic acid, 40% acetic acid and 10% hydrogen peroxide (1:1:2 ratio) on the hot plate at 90 °C for 1.5 h. Thirdly, the fiber was treated with 10% sodium hydroxide solution on the hot plate at 90 °C for 1 h. Finally, the fiber was bleached with 10% sodium hydroxide in 10% hydrogen peroxide at 90 °C for 1 h. In all stages, the ratios of KW to liquor used were 1:10. At the end of each stage, the fiber was filtered and washed several times with hot distilled water. The fiber obtained in the last stage was dried at 60 °C in an oven (Kottermann® 2711, Germany) and ground using a kitchen mill.

Nanofibrillation and aerogel formation

1% (w/w) cellulose dispersion in distilled water was first homogenized at 10,000 rpm for 5 min using a benchtop homogenizer (Pro Scientific, USA) and nanofibrillated using a VCX 750 ultrasonic processor (Sonics®, USA) at 40% amplitude for 4 h under an ice bath. The nanofiber was immediately placed in a refrigerator to be frozen using 5 mL plastic caps. Later, an aerogel was formed from frozen nanofibers after drying in a freeze-dryer (Operon Co., Ltd., Korea) at a temperature of -40 °C.

Determination of nanofibrillation degree

The nanofibrillation degree of ultrasonically processed fiber was determined according to the method of Campano *et al*.[7] According to this method, a concentration of 0.1% (w/w) nanofiber was prepared and centrifuged (Beckman Coulter Avanti J-20 XP Centrifuge, USA) at 4500 × g for 30 minutes. The ratio of the amount of nanofiber in the supernatant to the total amount of nanofiber was taken as nanofibillation degree.

Determination of chemical composition

The extracted cellulose fiber was investigated in terms of its composition, including the contents of cellulose, hemicelluloses, Klason lignin, and total ash, according to the methods described elsewhere.[6]

Drug loading and encapsulation efficiency determinations

An aqueous solution of diclofenac sodium was mixed with the nanofiber at a weight ratio of 3:1 (nanofiber:drug) and mixed at 350 rpm for 45 minutes using a magnetic stirrer (CIMAREC, Barnstead/Thermolyne). The drug–nanofiber mixture was then centrifuged (Beckman Coulter Avanti J-20 XP Centrifuge, USA) at 10,000 rpm and 20 °C for 20 minutes. The supernatant was collected and absorbance was measured at a wavelength of 276 nm using a UV/visible spectrophotometer (PG Instruments Limited, T92+, Leicestershire, UK). The drug loaded nanofiber was transferred into a 5 mL plastic cap, frozen and finally freeze-dried (Operon Co., Ltd, Korea). Drug loading capacity and encapsulation efficiency were determined using the following equations:[8]

$$\text{Drug loading capacity (\%)} = \frac{W_i - W_f}{A} \times 100 \quad (1)$$

$$\text{Encapsulation effeciency (\%)} = \frac{W_i - W_f}{W_i} \times 100 \quad (2)$$

where W_i and W_f are amount of drug added and the amount of drug quantified in the supernatant, respectively; A is the weight of the nanofiber used.

Characterization of the materials

Fourier–transform infrared (FTIR) spectroscopy analysis. The FTIR spectra of khat waste (KW), as-extracted cellulose (Cel), unloaded aerogel (ULA) and diclofenac sodium loaded aerogel (LA) were analyzed on a Spectrum 65 FT-IR (PerkinElmer) in the range of 4000-400 cm^{-1}, resolution 4 cm^{-1}, number of scans 4 using KBr pellets.

X-ray diffraction (XRD) analysis. XRD analyses of the samples were done using an XRD-7000 MAXima (Shimadzu, Japan) at 40 kV, 30 mA, with monochromatic Cu-Kα radiation. The scanning was carried out over an angular range from 10° to 40°. The crystalline indexes (CrI) of the samples were determined using the equation of Segal *et al*.[9]

$$\text{CrI} = [\,{}^{(I_{200} - I_{am})}/_{I_{200}}\,] \times 100 \quad (3)$$

where I_{200} is the maximum intensity of the diffraction from the 200 plane, and I_{am} is the intensity of the background scatter.

Thermogravimetric analysis (TGA) and differential scanning calorimetric (DSC) analysis. Both TGA and DSC analyses of the samples were performed using an SDT-Q600 Thermal Analyzer (TA Instrument, USA). This instrument simultaneously measures both TGA and DSC from a single sample. For TGA analysis, the samples were heated from room temperature to 700 °C at a heating rate of 10 °C/min and a nitrogen gas flow rate of 100 mL/min. For the DSC analysis, the temperature range from room temperature to 250 °C was used.

Scanning electron microscopy (SEM) analysis. Microscopic morphologies of the samples were determined using a scanning electron microscope (Tescan Vega 3 SBU, Brno, Czech Republic).

In vitro *drug release study.* The release of diclofenac sodium from LA was determined using a dissolution tester (Erweka DT 600, Germany) at temperature of 37 °C ± 0.5 °C, 100 rpm, pH 1.4 (2 h)

and then at pH 6.8 (for the next 4 h). The percent cumulative drug release was determined by measuring absorbance at the wavelength of 276 nm using a UV/visible spectrophotometer (PG Instruments Limited, T92+, Leicestershire, UK).

Data analysis. Data analysis was performed using the following software: Origin Pro 8.5.1, Origin Lab Corporation, MA, USA; ImageJ, National Institute of Health, USA; and Microsoft Excel 2016. Mean ± standard deviations were determined from three tests.

RESULTS AND DISCUSSION

Chemical composition of Cel and physical description of the materials

The extracted cellulose (Cel) was obtained from KW by using mild organic acids (formic acid and acetic acid), sodium hydroxide and hydrogen peroxide treatments in four stages. These chemicals have been used to extract cellulose from different biomasses. Formic acid depolymerizes lignin into low molecular-mass aromatics[10] and it can be used under relatively mild temperature,[11,12] can produce several reactive radicals, like HOO· and ·COOH in the presence of hydrogen peroxide, and can be recycled.[13,14] Acetic acid treatment removes hemicelluloses.[15] Sodium hydroxide treatment was used to dissolve lignin, residual hemicelluloses and pectin.[16] Hydrogen peroxide in alkaline condition solubilizes macromolecular hemicelluloses and also has delignifying and bleaching effects.[17]

Chemical composition analysis of Cel revealed the contents of cellulose (73.94%±4.34%), hemicelluloses (9.67%±2.89%), Klason lignin (15.35%±1.38%), and ash (1.04%±0.07%). From our previous work, KW contained cellulose (39.4%), hemicelluloses (12.75%), Klason lignin (28.67%), pectic matter (5.24%), fatty and waxy matter (7.87%), aqueous extractives (3.47%) and ash (3.4%).[18]

The macroscopic pictures of KW, Cel, ULA and LA are shown in Figure 1. Cel was white, fibrous, fluffy and odorless. ULA was colorless, folded like a plastic sheet, and light. LA, on the other hand, was greyish and slightly compact. In the nanofibrillation process, it was noticed that the color of the cellulose dispersion was changing from white to colorless due to the use of longer time for nanofibrillation (*i.e.*, 4 h).

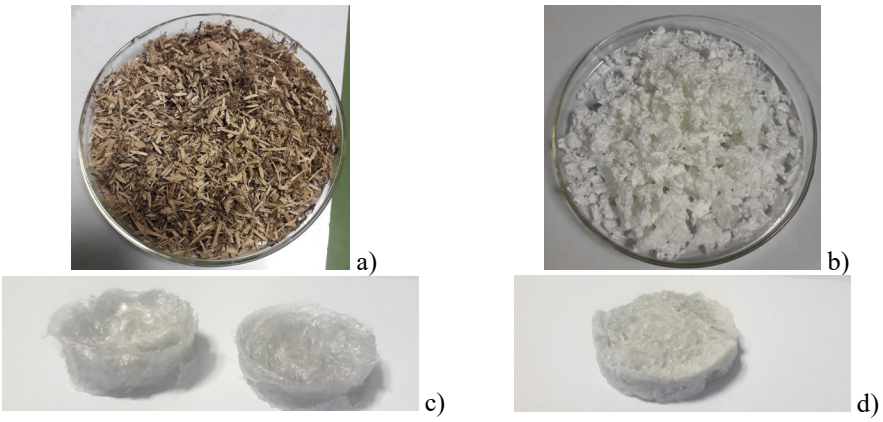

Figure 1: Photographs of a) KW (khat waste); b) Cel (as-extracted cellulose); c) ULA (unloaded aerogel); and d) LA (diclofenac sodium loaded aerogel)

Nanofibrillation degree

After nanofibrillation of Cel for 4 h, the nanofibrillation degree was determined to be 83.07%±0.5 (%). The high degree of nanofibrillation obtained in the present research could be due to the relatively longer time used to fibrillate the cellulose fiber. The higher degree of nanofibrillation can be indirectly inferred by observing the translucent color of ULA. A lower degree of nanofibrillation (*i.e.*, 35.2%) was obtained after homogenization of bacterial cellulose for 1 h.[7]

Drug loading capacity and drug encapsulation efficiency

In the present work, drug loading capacity and encapsulation efficiency of diclofenac sodium loaded aerogels were found to be 11.70%±2.64% and 35.11%± 7.91%, respectively. The value of drug loading capacity (11.7%) obtained in the present research was found to be lower when compared with the work done by Bhandari *et al*.[8] In their work, Bhandari *et a*l.[8] achieved a loading capacity of 18.98% for bendamustine

hydrochloride in an aerogel prepared from a commercial wood pulp nanofiber. A drug loading capacity of 18.98% was achieved by the above researchers when a nanofiber to drug ratio of 1:3 was used. In our work, the loading capacity of 11.7% was achieved when the nanofiber to drug ratio of 3:1 was used. In a study by Zhao *et al*.,[19] the sodium salicylate loading capacity of aerogels prepared from polyethyleneimine (PEI) grafted nanofibrillar bamboo pulp was found to be 78.00 mg/g. On the other hand, the unmodified aerogels of bamboo pulp had a loading capacity below 5 mg/g. The lower drug loading capacities of both PEI-modified and PEI-unmodified aerogels as compared to our work may be possibly explained by the fact that drug loading was performed after the formation of aerogels.

FTIR spectra

The FTIR spectra of KW, Cel, ULA, and LA are depicted in Figure 2. All samples have broad absorption peaks in the region of 3439-3338 cm^{-1}, which is due to OH in cellulose, hemicelluloses and lignin.[20] The band at about 2920 cm^{-1} and 2854 cm^{-1} of all samples is characteristic of CH stretching vibration of methyl and methylene groups.[21]

Unlike the other samples, KW has an absorption band at about 1744 cm^{-1}, which is ascribed to acetyl or uronic ester groups of hemicelluloses.[22] The peak at about 1600-1650 cm^{-1} is due to bending vibration of adsorbed water.[23]

The weak absorption peak found in all the samples at about 1377 cm^{-1} is due to C-H stretching of cellulose.[24] The peak at about 1338 cm^{-1} of Cel, ULA and LA is due to C-H ring in-plane bending vibrations of cellulose.[25] The weak band at about 1245 cm^{-1} of KW, which does not appear in the spectra of other samples is due to C-O stretching of acetyl group of lignin.[26]

The peak at around 1034 cm^{-1} is due to C-O-C pyranose ring stretching vibration in cellulose.[27] The band at 894 cm^{-1} of Cel could be due to β-glucosidic linkages between the anhydroglucose units of cellulose, confirming the structure of cellulose. The absorption peaks at about 1377 cm^{-1}, 1337 cm^{-1}, 1318 cm^{-1}, and 894 cm^{-1} are characteristic peaks of cellulose.[28]

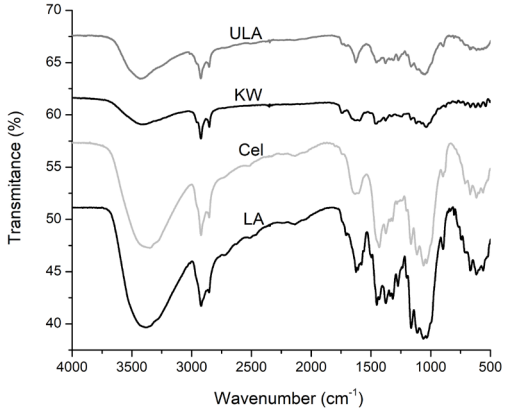

Figure 2: FTIR spectra of KW (khat waste), Cel (as-extracted cellulose), ULA (unloaded aerogel) and LA (diclofenac sodium loaded aerogel)

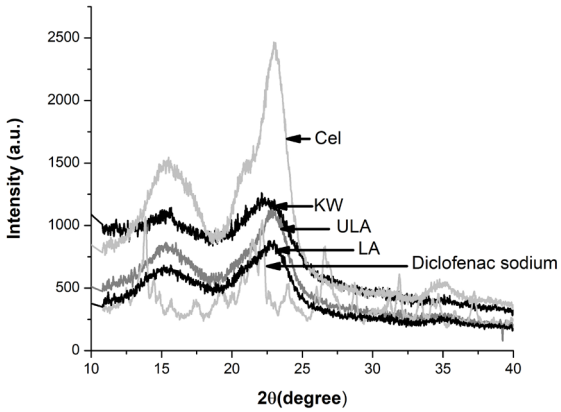

Figure 3: XRD patterns of KW (khat waste), Cel (as-extracted cellulose), ULA (unloaded aerogel) and LA (diclofenac sodium loaded aerogel)

XRD patterns of the samples

The XRD patterns of the samples are shown in Figure 3. The CrI of KW, Cel, ULA, and LA were determined to be 33.44%, 65.22%, 53.89%, and 49.37%, respectively. The higher CrI of Cel, as compared to KW, is an indication of the removal of the amorphous lignin and hemicelluloses from the KW due to the treatments. The CrI of ULA was lower than that of Cel. This might be due to the ultrasonic treatment of the Cel during nanofibrillation. For example, an aerogel produced from nanofibrillated cellulose of reed had lower CrI, as compared to native cellulose (*i.e*., 62.88% *vs* 67.42%).[29] The CrI of LA was lower than that of ULA. The XRD pattern of LA is similar to that of ULA, except that the CrI is lower in LA.

The presence of peaks for Cel at 2θ values of approximately 15.5°, 16.98°, 21.14°, 23.02°, and 34.74° was verified after first derivatization of the peaks and can be indexed to planes at (1-10), 110, 102, 200, and 004, respectively, indicating the Cel

is type Iβ.[30] The XRD intensities of diclofenac sodium is lower than those of ULA between 2θ values of 10º to 25.9º. This might be the reason for the lowering intensities of LA compared to ULA – an indirect indication of the presence diclofenac sodium in the LA.

TGA and DTG analyses

The TGA and DTG results of the materials are presented in Figure 4 and Figure 5, respectively, and the summarized results are presented in Table 1. Based on the thermal degradation pattern of the materials, the TGA plots can be divided into three thermogram regions (I, II, and III). All the samples had the lowest weight losses in region I and the highest weight losses in region II, whereas the weight losses were moderate in region III. In region I, ULA had the lowest weight loss (4.9%), while KW had the highest weight loss (10.8%). The weight losses in region I could be ascribed to evaporation of residual moisture from the samples.[31] Other studies also reported the occurrence of relatively high weight losses in untreated plant materials, as compared to extracted cellulose fiber in region I.[6]

As can be seen from Figure 4 and Table 1, all the materials had the highest weight losses in TGA region II. However, the materials had different onset of degradation and end of degradation temperatures. The temperature ranges from 245-370 °C for ULA to 225-355 °C for LA. Zhou *et al*.[32] reported that weight losses for nanofibrillated cellulose aerogels at 240-350 °C are caused by thermal degradation of cellulose. At a temperature of 400 °C (Table 1), the order for the residual weights was LA>KW>ULA>Cel. At the temperature of 700 °C, the residual weight of KW was slightly greater than that of ULA with percentages of 19.5 and 19.3, respectively. At the same temperature, the order for the residual weights was KW>ULA>LA>Cel. As can be seen from DTG plots, the rate of degradation of the materials is quite different. In the temperature range from 215 °C to 315 °C and beyond 445 °C, LA had the highest rate of thermal degradation. Contrary to this, beyond 485 °C, ULA had the lowest rate of thermal degradation. Moreover, the pattern of thermal degradation rate for ULA was similar to that of Cel, and that of LA with T_{max} of 351 °C, 343 °C and 332 °C, respectively. Interestingly, unlike the DTG plots of other samples, the DTG plot of LA also had a small peak at 286 °C, where there is a weight loss of 0.59%. This peak temperature corresponds to the melting point of diclofenac sodium.[33] Overall, the thermal stabilities of KW and ULA were almost equal and superior to those of Cel and LA. The high thermal stability of ULA makes it suitable for other applications, such as thermal insulation.[34]

DSC analysis

The DSC analysis results of the samples are shown in Figure 6. KW, Cel and LA demonstrated slight endothermic peaks at temperatures around 75 °C, 45 °C and 45 °C, respectively. The endothermic peaks for KW, Cel, ULA and LA at temperatures around 203-207 °C, 200-204 °C, 207-211 °C, and 201-204 °C, respectively, were also observed. This could be due to the melting of the crystalline region of the samples. However, these observed temperatures are lower than the onset degradation temperature of the samples seen in the TGA analysis results (Fig. 4).

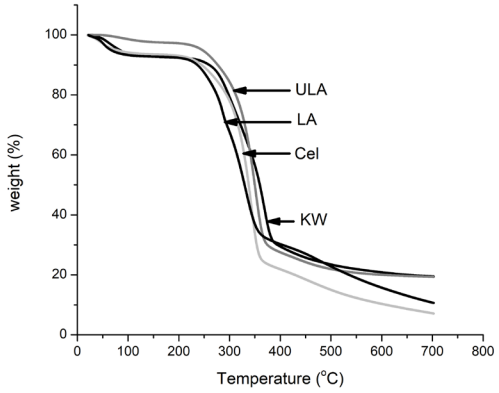

Figure 4: TGA plots of KW (khat waste), Cel (as-extracted cellulose), ULA (unloaded aerogel) and LA (diclofenac sodium loaded aerogel)

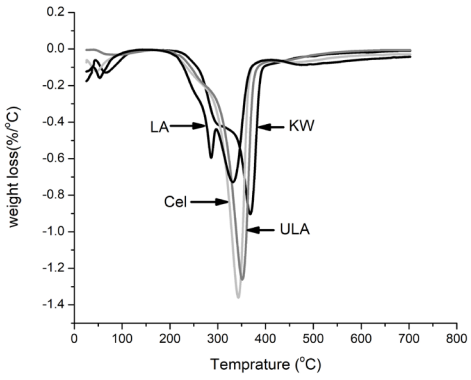

Figure 5: DTG plots of KW (khat waste), Cel (as-extracted cellulose), ULA (unloaded aerogel) and LA (diclofenac sodium loaded aerogel)

Table 1
Summary of TGA and DTG characterization of KW, Cel, ULA and LA

Material	Thermal degradation phase						
	TGA region I		TGA region II			TGA region III	
	T_{range} (°C)	Residue wt. (%)	T_{range} (°C)	T_{max} (°C)	Residue at 400 °C (%)	T_{range} (°C)	Residue at 700 °C (%)
KW	25-265	89.2	265-385	368	29.5	> 385	19.5
Cel	25-220	92.3	220-360	343	21.9	>360	7.2
ULA	25-245	95.1	245-370	351	27.5	>370	19.3
LA	25-225	91.2	225-355	332	30.2	>355	10.7

T_{range} – initial and final degradation temperature range; Residue wt. (%) – the weight of undegraded sample in percent; T_{max} is temperature of maximum degradation

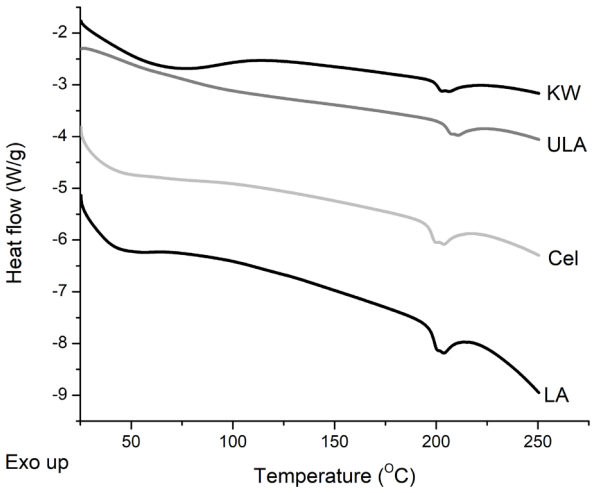

Figure 6: DSC plots of KW (khat waste), Cel (as extracted cellulose), ULA (unloaded aerogel) and LA (diclofenac sodium loaded aerogel)

As the temperature of DSC analysis increased, the endothermic heat of all the samples showed a decrease up to 250 °C and even until 750 °C (data not shown). The enthalpy of fusion (ΔH), as calculated for KW, Cel, ULA and LA, were determined to be 13.72 J/g, 25.37 J/g, 16.21 J/g and 26.88 J/g, respectively.

In our study, both ULA and LA produced endothermic peaks in the DSC plot, which indicated the fusion of the crystalline domain. However, in studies by Zhou *et al*.,[35] and Lopes *et al*.,[36] MCC aerogels prepared using ionic liquid did not produce a melting point under DSC analysis.

SEM analysis

The scanning electron micrograph images of KW, Cel, ULA and LA are shown in Figure 7. As can be seen from the SEM micrographs, KW is an intact material, with a measured average diameter of about 600 µm. Cel is fibrous, with measured diameters in the range from 9 to 16 µm. The removal of non-cellulosic components from KW can be also confirmed by the comparison of the micrographs of KW and Cel. The diameter of cellulose fiber from sisal was reported to be in the range of 7 to 31 µm, whereas that of unextracted sisal was 100 to 500 µm.[37] The micrograph image of ULA reveals its slightly rough surface, with scattered white spots of different size and shape. We speculate that the white spots could originate from unfibrillated cellulose fibers. On the other hand, the micrograph of LA shows it has relatively flat and sheet-like surface, as compared to that of ULA. The formation of a relatively more sheet-like surface for LA, as compared to ULA, might be attributed to the greater intermolecular attraction between diclofenac sodium and cellulose nanofibers, as compared to the intermolecular attractive force between cellulose nanofibers and water. Other researchers also showed that aerogels formed by the freeze drying method produced sheet-like surfaces.[38]

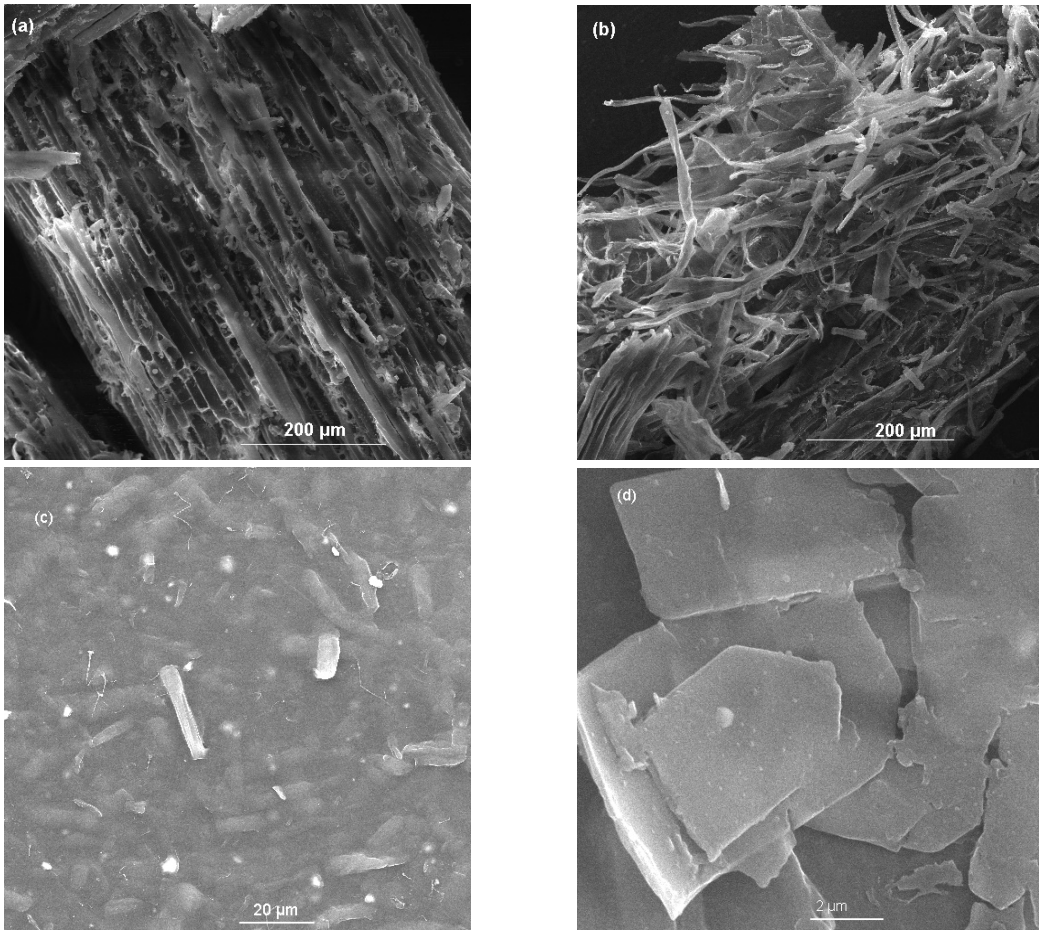

Figure 7: SEM images of (a) KW (khat waste) (scale bar 200 µm); (b) Cel (as-extracted cellulose) (scale bar 200 µm); (c) ULA (unloaded aerogel) (scale bar 20 µm); (d) pieces of LA (diclofenac sodium loaded aerogel (scale bar 2 µm)

***In vitro* drug release kinetics**

The release of diclofenac sodium from aerogels was observed in acidic medium (pH 1.4) for 2 h and subsequently for 4 h in basic medium (pH 6.8) to simulate the pH in the stomach and small intestine, respectively.

As can be seen from the graph in Figure 8, about 14% of the diclofenac sodium was released from the aerogel within 0.5 h and this could be due to the release of diclofenac sodium from the surface of the aerogels. About 22.6% and 31.4% of the drug was released within 5 h and 6 h, respectively, which indicates the drug sustaining effect of the aerogel. From the 5^{th} to the 6^{th} h of the testing, the highest successive drug release occurred and this may be due to softening of the aerogel.

In order to study the *in vitro* release kinetics of diclofenac sodium from the aerogel matrix, the data obtained were fitted to kinetic models, such as zero-order, first-order, Higuchi, Korsemayer-Peppas, and Hixson-Crowell models. The diclofenac sodium release data from the aerogel best fitted the Korsemayer-Peppas model, as it had the highest regression coefficient (R^2) value of 0.9008 (Table 2). The mechanism of diclofenac sodium release from the aerogel matrix was found by determining the release exponent (n) in the Korsemayer-Peppas model *via* linear regression of log cumulative percentage drug release *vs*. log time. The n value determined was found to be 0.1772. An n value less than 0.5 indicates that the drug transport mechanism is quasi-Fickian diffusion (partial diffusion).[39]

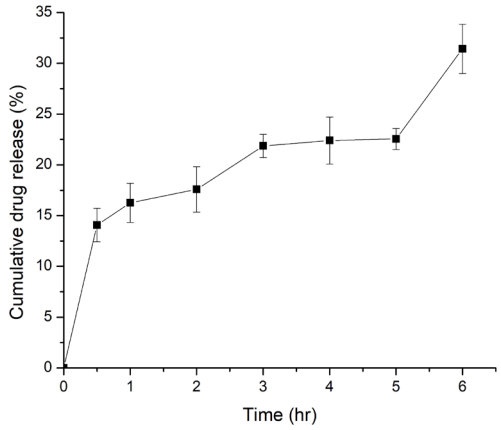

Figure 8: *In vitro* release pattern of diclofenac sodium from the loaded aerogel

Table 2
Summary of kinetic parameters obtained from diclofenac sodium release data fitted to different kinetic models

Zero order	First order	Higuchi	Korsmeyer-Peppas	Hixson-Crowell
$K_0 = 3.6954$	$K_1 = 0.0450$	$K_H = 10.4391$	$K_{KP} = 10.2428$	$K_{HC} = 0.0651$
$R^2 = 0.7509$	$R^2 = 0.7869$	$R^2 = 0.8959$	$R^2 = 0.9008$	$R^2 = 0.7760$
			n = 0.1772	

CONCLUSION

Nanofibrillation of the cellulose fiber obtained from khat waste for 4 h produced 83.07% nanofiber. The aerogel prepared was colorless, folded like a plastic sheet and light. The presence of FTIR absorption peaks for Cel at about 1377 cm^{-1}, 1337 cm^{-1}, 1318 cm^{-1}, and 894 cm^{-1} is characteristic of cellulose. The presence of peaks for Cel at 2θ values of approximately 15.5°, 16.98°, 21.14°, 23.02°, and 34.74°, as verified by first derivatization of the peaks, indicates Cel is Cellulose Iβ. The CrI of ULA was lower than that of Cel (53.89% *vs* 65.22%). TGA analysis revealed that ULA had higher thermal stability than Cel and LA. The aerogel was able to load 11.7 mg of diclofenac sodium per 100 mg of nanofiber and encapsulated about 35.11% of the incorporated drug. Less than one-third (*i.e.* 31.4%) of the incorporated drug was released within 6 h.

ACKNOWLEDGMENTS: The authors acknowledge the Department of Pharmaceutics and Social Pharmacy, School of Pharmacy, College of Health Sciences, Addis Ababa University, for access to laboratory facilities. We also extend our gratitude to Dr. Nisha Marry Joseph for facilitating SEM analysis. One of the authors (T.G.) acknowledges Tri Sustain Project, Germany, for financial assistance provided during his PhD study.

REFERENCES

[1] C. Tan, B. M. Fung, J. K. Newman and C. Vu, *Adv. Mater.*, **13**, 644 (2001), https://doi.org/10.1002/1521-4095(200105)13:9<644::AID-ADMA644>3.0.CO;2-%23

[2] C. Aulin, J. Netrval, L. Wågberg and T. Lindstrom, *Soft Matter*, **6**, 3298 (2010), https://doi.org/10.1039/C001939A

[3] L. Y. Long, Y. X. Weng and Y. Z. Wang, *Polymers* (*Basel*),**10**, 623 (2018), https://doi.org/10.3390/polym10060623

[4] B. T. Mekonnen, W. Ding, H. Liu, S. Guo, X. Pang *et al*., *J. Leather Sci. Eng.* **3**, 25 (2021), https://doi.org/10.1186/s42825-021-00067-y

[5] A. C. Pierre and G. M. Pajonk, *Chem. Rev.*, **102**, 11 (2002), https://doi.org/10.1021/cr0101306

[6] T. Gabriel, A. Belete, F. Syrowatka, R. H. H. Neubert and T. Gebre-Mariam, *Int. J. Biol. Macromol.*, **158**, 1248 (2020), https://doi.org/10.1016/j.ijbiomac.2020.04.264

[7] C. Campano, N. Merayo, C. Negro and A. Blanco, *Int. J. Biol. Macromol.*, **114**, 1077 (2018), https://doi.org/10.1016/j.ijbiomac.2018.03.170

[8] J. Bhandari, H. Mishra, P. K. Mishra, R. Wimmer and F. J. Ahmad *et al*., *Int. J. Nanomed.*, **12**, 2021 (2017), https://doi.org/10.2147/IJN.S124318

[9] L. Segal, J. J. Creely, A. E. Martin and C. M. Conrad, *Text. Res. J.*, **29**, 10 (1959), https://doi.org/10.1177/004051755902901003

[10] Y. Feng, G. Li, X. Li, N. Zhu, B. Xiao *et al*., *Bioresour. Technol.*, **214**, 520 (2016), https://doi.org/10.1016/j.biortech.2016.04.137

[11] J. S. Kim, Y. Y. Lee and T. H. Kim, *Bioresour. Technol.*, **199**, 42 (2016), https://doi.org/10.1016/j.biortech.2015.08.085

[12] K. Zhang, Z. Pei and D. Wang, *Bioresour. Technol.*, **199**, 21 (2016), https://doi.org/10.1016/j.biortech.2015.08.102
[13] N. K. V. Leitner and M. Dore, *J. Photochem. Photobiol. A Chem.*, **99**, 137 (1996), https://doi.org/10.1016/S1010-6030(96)04360-2
[14] S. M. Davies, R. S. Linforth, S. J. Wilkinson, K. A. Smart and D. Cook, *J. Biotechnol. Biofuels*, **4**, 28 (2011), https://doi.org/10.1186/1754-6834-4-28
[15] V. P. Kommula, K. O. Reddy, M. Shukla, T. Marwala, E. V. S. Reddy *et al.*, *Int. J. Polym. Anal. Charact.*, **21**, 18 (2016)
[16] A. Orue, A. Jauregi, U. Unsuain, J. Labidi, A. Eceiza *et al.*, *Compos. Part A Appl. Sci. Manuf.*, **84**, 186 (2016), https://doi.org/10.1016/j.compositesa.2016.01.021
[17] R. C. Sun, J. Tomkinson, S. Q. Wang and W. Zhu, *Polym. Degrad. Stab.*, **67**, 101 (2000)
[18] T. Gabriel, K. Wondu and J. Dilebo, *PLoS One*, **16** (2021), https://doi.org/10.1371/journal.pone.0246794
[19] J. Zhao, C. Lu, X. He, X. Zhang, W. Zhang *et al.*, *ACS Appl. Mater. Interfaces*, **7**, 2607 (2015), https://doi.org/10.1021/am507601m
[20] J. Astruc, M. Nagalakshmaiah, G. Laroche, M. Grandbois, S. Elkoun *et al.*, *Carbohyd. Polym.*, **178**, 352 (2017), https://doi.org/10.1016/j.carbpol.2017.08.138
[21] S. Naduparambath and E. Purushothaman, *Cellulose*, **23**, 1803 (2016), https://doi.org/10.1007/s10570-016-0904-3
[22] E. Tezcan and O. G. Atıcı, *Waste Manag.*, **70**, 181 (2017), https://doi.org/10.1016/j.wasman.2017.09.017
[23] M. Asrofi, H. Abral, A. Kasim and A. Pratoto, *J. Metastable Nanocryst. Mater.*, **29**, 9 (2017), https://doi.org/10.4028/www.scientific.net/JMNM.29.9
[24] A. Nabili, A. Fattoum, R. Passas and E. Elaloui, *Cellulose Chem. Technol.*, **50**, 1015 (2016), https://www.cellulosechemtechnol.ro/pdf/CCT9-10(2016)/p.1015-1023.pdf
[25] P. K. Adapa, L. G. Tabil, G. J. Schoenau, T. Canam and T. Dumonceaux, *J. Agric. Sci. Technol.*, **B1**, 177 (2011), https://core.ac.uk/download/pdf/154487195.pdf
[26] H. Suryanto, A. A. Fikri, A. A. Permanasari, U. Yanuhar and S. Sukardi, *J. Nat. Fibers*, **15**, 012145 (2018), https://doi.org/10.1088/1757-899X/1034/1/012145
[27] B. Soni, E. B. Hassana and B. Mahmoud, *Carbohyd. Polym.*, **134**, 581 (2015), https://doi.org/10.1016/j.carbpol.2015.08.031
[28] M. S. Yeasmin and I. H. Mondal, *Int. J. Biol. Macromol.*, **80**, 725 (2015), https://doi.org/10.1016/j.ijbiomac.2015.07.040
[29] Y. Jiao, C. Wan, T. Qiang and J. Li, *Appl. Phys. A.*, **122**, 686 (2016), https://doi.org/10.1007/s00339-016-0194-5
[30] G. SriBala, R. Chennuru, S. Mahapatra and R. Vinu, *Cellulose*, **23**, 8714 (2016), https://doi.org/10.1021/ie5007905
[31] C. Wan, Y. Lu, Y. Jiao, C. Jin, Q. Sun *et al.*, *J. Appl. Polym. Sci.*, **132**, 42037 (2015)
[32] Z. Zhou, X. Zhang, C. Lu, L. Lan and G. Yuan, *RSC Adv.*, **4**, 8966 (2014), https://doi.org/10.1039/C3RA46441E
[33] P. Tudja, M. Z. Khan, E. Mestrović, M. Horvat and P. Golja, *Chem. Pharm. Bull.*, **49**, 1245 (2001), https://doi.org/10.1248/cpb.49.1245
[34] H. Liao, H. Zhang, H. Hong, Z. Li, Y. Lin *et al.*, *J. Membr. Sci.*, **514**, 332 (2016)
[35] Z. Zhou, X. Zhang, C. Lu, L. Lan and G. Yuan, *RSC Adv.*, **4**, 8966 (2014), https://doi.org/10.1039/C3RA46441E
[36] J. M. Lopes, A. N. Mustapa, M. Pantić, M. D. Bermejo, Á. Martín *et al.*, *J. Supercrit. Fluids*, **130**, 17 (2017), https://doi.org/10.1016/j.supflu.2017.07.018
[37] J. I. Morán, V. A. Alvarez, V. P. Cyras and A. Vázquez, *Cellulose*, **15**, 149 (2008), https://doi.org/10.1007/s10570-007-9145-9.
[38] C. Jiménez-Saelices, B. Seantier, B. Cathala and Y. Grohens, *Carbohyd. Polym.*, **157**, 105 (2017), https://doi.org/10.1016/j.carbpol.2016.09.068
[39] M.-C. Rosu and I. Bratu, *Prog. Nat. Sci.*: *Mater.*, **24**, 205 (2014), https://doi.org/10.1016/j.pnsc.2014.05.007